JOURNAL OF AGRICULTURAL AND FOOD CHEMISTRY

pubs.acs.org/JAFC

Article

Discovery and Characterization of Phenolic Compounds in Bearberry (*Arctostaphylos uva-ursi*) Leaves Using Liquid Chromatography−Ion Mobility−High-Resolution Mass Spectrometry

Xue-Chao Song, Elena Canellas, Nicola Dreolin, Cristina Nerin,* and Jeff Goshawk

Cite This: *J. Agric. Food Chem.* 2021, 69, 10856−10868

Read Online

ACCESS | Metrics & More | Article Recommendations | Supporting Information

ABSTRACT: The characterization and quantification of phenolic compounds in bearberry leaves were performed using hyphenated ion mobility spectroscopy (IMS) and a quadrupole time-of-flight mass spectrometer. A higher identification confidence level was obtained by comparing the measured collision cross section ($^{TW}CCS_{N2}$) with predicted values using a machine learning algorithm. A total of 88 compounds were identified, including 14 arbutin derivatives, 33 hydrolyzable tannins, 6 flavanols, 26 flavonols, 9 saccharide derivatives, and glycosidic compounds. Those most reliably reproduced in all samples were quantified against respective standards. Arbutin (47−107 mg/g), 1,2,3,4,6-pentagalloylglucose (6.6−12.9 mg/g), and quercetin 3-galactoside/quercetin 3-glucoside (2.7−5.7 mg/g) were the most abundant phenolic components in the leaves. Quinic acid and ellagic acid were also detected at relatively high concentrations. The antioxidant activity of the most abundant compounds was evaluated. A critical view of the advantages and limitations of traveling wave IMS and CCS for the discovery of natural products is given.

KEYWORDS: *collision cross section, ion mobility, mass spectrometry, bearberry, phenolic compounds*

1. INTRODUCTION

Arctostaphylos uva-ursi, also known as bearberry, is a wild shrub in the genus *Arctostaphylos*, belonging to the Ehododendron family. This plant is mainly found in Europe, Asia, and North America.[1] Over recent decades, many studies have shown that *Arctostaphylos uva-ursi* extracts possess remarkable antioxidant, antimicrobial, and anti-inflammatory properties.[2−4] *Arctostaphylos uva-ursi* leaf extracts have been used as a skin-whitening agent, as well as antioxidant agents in food and food packaging formulations.[5−7] The health benefits can be attributed to bioactive components, which include arbutin, flavonols, flavanols, and phenolic acids. The phenolic compounds in bearberry leaves have been tentatively characterized in previous studies,[5,8−10] in which the techniques of photodiode array (PDA) and time-of-flight mass spectrometry (Tof/MS) were used, and compound identification was mainly based on retention time (RT), *m*/*z*, and fragmentation pathway analysis. The presence of isomers and lack of reference standards limited the complete elucidation of such components and many remain unconfirmed. Furthermore, chromatographic coelution of structurally similar compounds yields complex mass spectra that are extremely challenging and time consuming to interpret. The inclusion of an additional dimension of separation can aid in increasing peak capacity and improving the identification confidence when analyzing such complex matrices.[11,12]

In recent years, ultrahigh performance liquid chromatography (UPLC) coupled to ion mobility spectroscopy (IMS) and a quadrupole time-of-flight mass spectrometer (UPLC-IMS-QTof) has been shown to be a powerful technique for the untargeted screening of complex samples.[13−17] The ionized molecules pass through a drift cell under an electric field and collide with a buffer gas of neutral molecules (normally nitrogen or helium). The arrival time of the ionized molecules is related to their size, charge, and shape,[18] and as such, IMS potentially allows the separation of isobaric and isomeric compounds that coelute in liquid chromatography. Following ion-mobility separation, the ions undergo a collision-induced dissociation (CID) which ensures that a precursor ion and its corresponding product ions have the same arrival time. The alignment of precursor and fragment ions based on both RT and arrival time dimensions dramatically reduces the number of ions that do not belong to the candidate of interest (e.g., ions belonging to matrix interferences or coeluting compounds) and provides much cleaner mass spectra.

Unlike the direct determination of rotationally averaged collision cross sections (CCSs) in drift tube IMS (DTIMS), the CCS values are derived from the arrival time of ionized species via a power-law calibration in traveling wave IMS (TWIMS); the calibration was performed by using a set of reference compounds (always polyalanine) with known CCS values. The CCS represents a unique physicochemical parameter of a molecule, which is associated with the size, shape, and charge of ions. Unlike the arrival time, the CCS is a stable parameter, which has been proven to be transferrable between different systems, different laboratories, and different

Received: May 13, 2021
Revised: July 8, 2021
Accepted: August 5, 2021
Published: September 8, 2021

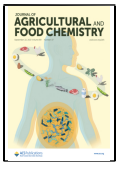

https://doi.org/10.1021/acs.jafc.1c02845
J. Agric. Food Chem. 2021, 69, 10856−10868

experimental conditions, provided that the same calibration procedure is applied.[19−21] Therefore, the CCS can be treated as an additional structural descriptor for compound identification.[22]

In this work, we explore the potential benefits of including CCS values within the compound elucidation process, in order to assess the capabilities of a hyphenated technique for high throughput phenolic compound discovery. The reference CCS values were obtained either from the existing literature or from open-source machine-learning prediction models. Phenolic compounds, confirmed using reference standards, were quantified to evaluate their distributions in nine bearberry leaves from different geographic origins. The antioxidant activity of these compounds was also evaluated to assess the contribution to the total antioxidant capacity of bearberry leaf derivatives.

2. MATERIALS AND METHODS

2.1. Plant Samples. Nine *Arctostaphylos uva-ursi* leaf samples were collected from three provinces of Spain. Detailed information of locations (latitude and altitude) and sampling seasons have been described in the previous work.[5] A representative sample from each location was prepared by mixing all the leaves collected from that specific sampling point. After collection, the leaves were dried in an oven at 60 °C for 24 h, ground into powder, and stored in a refrigerator at 4 °C until further analysis.

2.2. Chemicals. Arbutin (≥98%, CAS: 497-76-7), gallic acid (CAS: 149-91-7), ellagic acid (CAS: 476-66-4), ferulic acid (≥98%, CAS: 1135-24-6), *p*-coumaric acid (≥98%, CAS: 501-98-4), chlorogenic acid (≥95%, CAS: 327-97-9), (−)-quinic acid (≥98%, CAS: 77-95-2), caffeic acid (≥98%, CAS: 331-39-5), carnosol (≥98%, CAS: 5957-80-2), rosmarinic acid (≥97%, 20283-92-5), sinapinic acid (≥98%, CAS: 530-59-6), hydroquinone (≥99%, CAS: 123-31-9), propyl gallate (CAS: 121-79-9), morin (≥90%, CAS: 480-16-0), oleuropein (≥98%, 32619-42-4), glycitein 7-glucoside (CAS: 40246-10-4), myricetin (≥96%, CAS: 529-44-2), quercetin (≥98%, CAS: 117-39-5), kaempferol (≥97%, CAS: 520-18-3), silibinin (≥98%, CAS: 22888-70-6), quercetin 3-rhamnoside (CAS: 522-12-3), quercetin 3-glucoside (CAS: 482-35-9), quercetin 3-galactoside (≥97%, CAS: 482-36-0), myricetin 3-rhamnoside (≥99%, CAS: 17912-87-7), luteolin 7-glucoside (≥98%, CAS: 5373-11-5), (−)-epicatechin (>97%, CAS: 490-46-0), (+)-catechin (≥99%, CAS: 154-23-4), (−)-epigallocatechin gallate (≥95%, CAS: 989-51-5), D-(+)-glucose (≥99%, CAS: 50-99-7), (+)-lactose(≥99%, CAS: 63-42-3), D-(+)-trehalose (≥99%, CAS: 99-20-7), and formic acid (≥98.0%, CAS: 64-18-6) were obtained from Sigma-Aldrich Química S.A. (Madrid, Spain). (−)-Epicatechin gallate (CAS: 1257-08-5) and 1,2,3,4,6-penta-*O*-galloyl-*β*-D-glucose (CAS: 14937-32-7) were obtained from Cayman chemical company (Ann Arbor, Michigan, USA). HPLC grade ethanol (≥99.9%) and methanol (≥99.9%) were purchased from Scharlau Chemie S.A (Sentmenat, Spain). Deionized water used for all the solutions and dilutions was obtained from a Millipore Milli-QPLUS 185 system (Madrid, Spain).

Standard stock solutions of all compounds were prepared in methanol at a concentration of 1000 mg/kg, with the exception of ellagic acid, which was dissolved in dimethyl sulfoxide. Mixed standard working solutions, of different concentrations, were produced by diluting the stock solutions with the appropriate amount of 70% ethanol (v/v). All the standard solutions were prepared under gravimetric control to accurately maintain the concentrations and were kept at −20 °C until analysis.

2.3. Extraction of *Arctostaphylos uva-ursi* Leaves. The method used to extract the phenolic compounds from *Arctostaphylos uva-ursi* leaves was based on that described in a previous study[5] with some modifications. Briefly, 0.1 ± 0.01 g of leaf powder was placed in a 20 mL glass vial, 10 g of 70% ethanol (v/v) was added, and the vial was agitated in an ultrasound-assisted bath for 30 min at 100 W. The sample was then centrifuged for 20 min at 4000g_n. A portion of the supernatant was filtered through a 0.22 μm nylon membrane directly into an LC vial for analysis. The remainder was stored at 4 °C.

2.4. UPLC-IMS-QT Analysis. An Acquity I-Class UPLC system (with a Flow Through Needle sample manager) coupled to a Vion IMS-QTof mass spectrometer with an electrospray ionization (ESI) source (Waters, Manchester, UK) was employed for all analyses in this study. The chromatographic separation was carried out on a CORTECS C18 UPLC column (2.1 × 100 mm, 1.6 μm particle size, 90 Å pore size) at a flow rate of 0.3 mL/min. The mobile phase consisted of water (A) and methanol (B), both with 0.1% formic acid (v/v). The LC gradient followed a ramp from 5 to 100% B for the first 7 min, was isocratic at 100% B from 7 to 11 min, returned to the initial conditions (5% B) from 11 to 11.1 min, and then re-equilibrated at 5% B from 11.1 to 13 min. The injection volume was 10 μL, and the sample and column temperature were maintained at 10 and 40 °C, respectively.

The mass spectrometer was operated in negative ion mode over the mass range 50−1000 m/z with a scan time of 0.2 s. Capillary and cone voltages were −1 kV and 30 V, respectively. The source temperature was set at 120 °C, and the cone gas flow rate was 50 L/h. N_2 was used as the desolvation gas at a flow rate of 800 L/min and a temperature of 500 °C. Data were acquired in high definition MS^E mode ($HDMS^E$), in which the instrument switches between two energy states (low energy: 6 eV, high energy: ramp 20−40 eV) to obtain precursor and product ion information in separate spectra but within a single acquisition. Because the ion mobility cell is positioned before the collision chamber in the Vion IMS-Qtof mass spectrometer, the precursor ion and its corresponding fragments have the same arrival time. Leucine−Enkephalin ($[M - H]^-$ ion, m/z 554.2620), at a concentration of 100 ng/mL and infused at a rate of 15 μL/min through a LockSpray channel, was used for real-time mass correction. The IMS gas flow rate was 25 mL/min with a wave velocity of 250 m/s and an IMS pulse height of 45 V. Data acquisition and processing were carried out on UNIFI v.1.9 Scientific Information System (Waters, Manchester, UK).

Major Mix IMS/Tof Calibration Kit (ref. 186008113, Waters, Wilmslow, UK) was used for the CCS calibration of Vion instruments. The detailed information about the calibration substances and their CCS values is shown in Table S1. A Test-Mix solution was injected after each batch of 10 standard injections to monitor the stability of the system. Table S2 shows m/z and CCS values for each compound in the Test-Mix. For stability, it was ensured that the variation in the m/z and CCS measurements was less than 5 ppm and less than 2%, respectively.

2.5. Identification Workflow. Thirty-three standards, which included phenolic acids, flavonols, and flavanols, were analyzed using the conditions mentioned above. The m/z values, adducts, RT, CCS values, and fragment ions were added to an in-house database. The leaf samples were subsequently screened against the in-house library created from the phenolic standards. The criteria used to match a target to a component in the data were: RT < 0.1 min, mass error <5 ppm, CCS delta <2%, and for at least one fragment ion to be found.

In addition to the targeted screen, a visual inspection of the data was performed using the base peak intensity (BPI) chromatograms, and a binary comparison between a blank and a sample was performed within UNIFI to determine unidentified peaks unique to the sample. The Multivariate Analysis tool in UNIFI was also used to determine whether there were any low-intensity compounds, unique to the samples, that were masked by the background present in full scan chromatograms. A list of markers unique to the samples was generated with each marker uniquely defined by an m/z value, an RT, and an arrival time. The markers were subsequently analyzed using the Discovery Tool in UNIFI, which links together elemental composition calculations, online ChemSpider database searching, and fragment match, in which substructures generated from the structure of a candidate compound are matched to ions in the high energy data.

Elemental compositions were derived for the precursor ion of each marker using the elements C, H, and O because most phenolic derivatives consist of just these three elements. Two criteria were used

https://doi.org/10.1021/acs.jafc.1c02845
J. Agric. Food Chem. 2021, 69, 10856−10868

Table 1. Phenolic Compounds Identified in Bearberry Leaves in Electrospray Negative Ion Mode[a]

no.	RT (min)	measured CCS (Å^2)	reference CCS (Å^2)	m/z observed	fragments	molecular formula	candidate name	mass error (ppm)	confidence level
1	0.74	133.67	133.22	191.0562	127.0401, 108.0215, 85.0295	$C_7H_{12}O_6$	quinic acid	0.42	1
2	0.84	161.42		295.1031		$C_{11}H_{20}O_9$	unknown	−1.24	4
3	0.84	172.71	168	331.0667	271.0456, 211.0244, 169.0139, 125.0242	$C_{13}H_{16}O_{10}$	galloyl glucose	−1.18	3
4	0.84	206.62		493.1194	323.0988, 161.0457	$C_{19}H_{26}O_{15}$	galloyl di-hexoside	−0.98	3
5	0.85	194.11	191	483.0774	331.0669, 169.0139	$C_{20}H_{20}O_{14}$	digalloyl glucose	−1.19	3
6	0.86	172.13	172.74	271.0819	108.0215	$C_{12}H_{16}O_7$	arbutin	−1.62	1
7	0.95	124.04	123.83	169.014	125.0242	$C_7H_6O_5$	gallic acid	−1.32	1
8	1.21	188.06		389.1084	347.0979	$C_{16}H_{22}O_{11}$	unknown	−1.40	4
9	1.24	173.49	168	331.0665	271.0451, 211.0244, 169.0138, 125.0242	$C_{13}H_{16}O_{10}$	galloyl glucose	−1.75	3
10	1.36	170.53	168	331.0669	169.0142, 125.0242	$C_{13}H_{16}O_{10}$	galloyl glucose	−0.63	3
11	1.52	170.88	168	331.0669	271.0461, 211.0247, 169.0142	$C_{13}H_{16}O_{10}$	galloyl glucose	−0.63	3
12	1.57	172.33		325.0563	169.0141, 125.0242	$C_{14}H_{14}O_9$	galloylshikimic acid	−0.59	3
13	1.67	193.78	191	483.0776	331.0669	$C_{20}H_{20}O_{14}$	digalloyl glucose	−0.89	3
14	1.69	160.88		295.1031		$C_{11}H_{20}O_9$	unknown	−1.03	4
15	1.78	170.17		315.0718	152.0113, 108.0216	$C_{13}H_{16}O_9$	unknown	−0.10	4
16	1.79	203.65		423.0928	313.0561, 169.0140, 125.0241	$C_{19}H_{20}O_{11}$	galloyl arbutin	−1.12	3
17	1.95	202.77		423.0928	313.0562, 169.0140	$C_{19}H_{20}O_{11}$	galloyl arbutin	−1.12	3
18	1.95	172.19		325.0562	169.0141, 125.0242	$C_{14}H_{14}O_9$	galloylshikimic acid	−0.89	3
19	2.03	192.99	191	483.0776	271.0459	$C_{20}H_{20}O_{14}$	digalloyl glucose	−0.82	3
20	2.07	225.49	220	635.0887	407.0774, 289.0719	$C_{27}H_{24}O_{18}$	trigalloyl glucose	−0.48	3
21	2.12	203.74		423.0927	313.0561, 169.0140, 125.0241	$C_{19}H_{20}O_{11}$	galloyl arbutin	−1.43	3
22	2.18	192.89	191	483.0772	245.0453	$C_{20}H_{20}O_{14}$	digalloyl glucose	−1.65	3
23	2.22	183.12	168.10	343.1031	135.0449	$C_{14}H_{18}O_7$	picein	−1.29	2
24	2.25	233.13	220	635.0886	465.0671	$C_{27}H_{24}O_{18}$	trigalloyl glucose	−0.69	3
25	2.28	300.59		951.0745		$C_{41}H_{28}O_{27}$	geraniin isomer	−0.04	3
26	2.34	221.29	220	635.0886	483.0774, 271.0457, 169.0140	$C_{27}H_{24}O_{18}$	trigalloyl glucose	−0.58	3
27	2.35	193.08	191	483.0775	331.0673, 271.0457, 211.0246	$C_{20}H_{20}O_{14}$	digalloyl glucose	−1.11	3
28	2.35	156.61	157.25	289.0714	245.0817, 203.0711, 137.0242, 109.0290	$C_{15}H_{14}O_6$	(+)-catechin	−1.39	1
29	2.39	183.77		423.0928	313.0559, 169.0140, 151,0035, 125,0241	$C_{19}H_{20}O_{11}$	galloyl arbutin	−1.17	3
30	2.46	168.93	170.70	313.0925	273.0037, 247.0244, 151.0400, 108.0215	$C_{14}H_{18}O_8$	6-*O*-acetylarbutin	−1.25	2
31	2.49	172.66		359.1344	182.0576, 151.0399	$C_{16}H_{24}O_9$	unknown	−1.10	4
32	2.51	299.96		951.0745	933.0650, 463.0508, 300.9988, 273.0036	$C_{41}H_{28}O_{27}$	geraniin isomer	0.00	3
33	2.55	180.53		423.0930	261.0401, 151.0035, 123.0086, 108.0215	$C_{19}H_{20}O_{11}$	tetrahydroxy-glucopyranosyloxy-benzophenone	−0.60	3
34	2.64	249.56		729.1457	407.0773, 289.0717	$C_{37}H_{30}O_{16}$	procyanidin gallate	−0.57	3
35	2.66	195.49		477.0667	271.0459	$C_{21}H_{18}O_{13}$	quercetin glucuronide	−1.62	3
36	2.67	200.48	198.8	457.0773	169.0141	$C_{22}H_{18}O_{11}$	(−)-epigallocatechin gallate	−0.80	1
37	2.68	270.27	264	787.0997		$C_{34}H_{28}O_{22}$	tetragalloyl glucose	−0.26	4
38	2.69	224.53	220	635.0884	465.0669, 313.0562, 169.0141	$C_{27}H_{24}O_{18}$	trigalloyl glucose	−0.90	3
39	2.76	221.94	222	633.0734	463.0513, 300.9989, 275.0196	$C_{27}H_{22}O_{18}$	corilagin	0.11	2
40	2.81	282.73		881.1571	729.1438, 559.1251, 407.0774, 289.0716	$C_{44}H_{34}O_{20}$	procyanidin di-gallate	0.07	3
41	2.82	204.29		447.1506	269.1026, 137.0242	$C_{19}H_{28}O_{12}$	glucopyranosyl methyl arbutin	−0.54	3
42	2.82	195.59		477.0673		$C_{21}H_{18}O_{13}$	quercetin glucuronide	−0.30	4
43	2.84	156.54	156.54	289.0716	245.0820, 109.0289	$C_{15}H_{14}O_6$	(−)-epicatechin	−0.50	1
44	2.92	170.4		323.1346	203.0350, 166.0631	$C_{13}H_{24}O_9$	unknown	−0.51	4
45	2.93	215.24		575.1038	423.0930, 465.0670, 313.0564	$C_{26}H_{24}O_{15}$	digalloyl arbutin	−0.70	3
46	2.93	304.37		965.0908		$C_{42}H_{30}O_{27}$	unknown	0.66	4
47	3.01	266.22	264	787.1003	635.0892,617.0782, 465.0670, 447.0568, 313.0563, 169.0141	$C_{34}H_{28}O_{22}$	tetragalloyl glucose	0.39	3

https://doi.org/10.1021/acs.jafc.1c02845
J. Agric. Food Chem. 2021, 69, 10856−10868

Table 1. continued

no.	RT (min)	measured CCS (Å^2)	reference CCS (Å^2)	m/z observed	fragments	molecular formula	candidate name	mass error (ppm)	confidence level
48	3.05	212.07		575.1041	423.0930, 261.0395, 151.0035	$C_{26}H_{24}O_{15}$	digalloyl arbutin	−0.28	3
49	3.12	215.13		445.1716	327.1245, 179.0561, 161.0459	$C_{20}H_{30}O_{11}$	unknown	0.08	3
50	3.19	198.42	196.87	441.0828	289.0719, 169.0143, 125.0244	$C_{22}H_{18}O_{10}$	(−)-epicatechin 3-gallate	0.21	1
51	3.21	220.57		575.1045	423.0934, 169.0143	$C_{26}H_{24}O_{15}$	digalloyl arbutin	0.51	3
52	3.28	247.3		727.1155	575.1048, 557.0946, 405.0819	$C_{33}H_{28}O_{19}$	trigalloyl arbutin	0.48	3
53	3.29	195.91	200.50	437.1088	313.0564, 241.0351, 168.0062, 123.0085	$C_{20}H_{22}O_{11}$	6″-galloyl methyl arbutin	−0.31	3
54	3.30	137.63	141.00	197.0454	169.0141, 124.0163	$C_9H_{10}O_5$	ethyl gallate	−0.54	2
55	3.30	209.43		461.1662	131.0347, 191.0563	$C_{20}H_{30}O_{12}$	unknown	−0.58	4
56	3.35	266.49	264	787.0995	618.0821	$C_{34}H_{28}O_{22}$	tetragalloyl glucose	−0.59	3
57	3.35	289.19	292.00	939.1108	787.0998, 769.0889, 617.0785, 599.0690, 465.0676	$C_{41}H_{32}O_{26}$	1,2,3,4,6-pentagalloyl glucose	−0.09	1
58	3.36	195.32	196.70	465.1035	313.0952, 303.0514, 285.0414, 151.0401	$C_{21}H_{22}O_{12}$	taxifolin 3-glucoside	−0.64	2
59	3.37	205.92		493.0622	315.0150	$C_{21}H_{18}O_{14}$	myricetin glucuronide	−0.36	3
60	3.38	193.22	190	433.0409	391.1023, 313.0952, 175.0398	$C_{19}H_{14}O_{12}$	ellagic acid pentoside	−0.87	3
61	3.43	202.60		479.0833	316.0226, 287.0197, 271.0248,	$C_{21}H_{20}O_{13}$	myricetin hexoside	0.39	3
62	3.51	302.27		955.1064		$C_{41}H_{32}O_{27}$	unknown	0.65	4
63	3.55	222.00		615.0991	463.0879, 313.0565, 301.0346, 169.0142	$C_{28}H_{24}O_{16}$	galloyl-quercetin-hexoside	−0.14	3
64	3.56	196.65		477.1037	299.0200	$C_{22}H_{22}O_{12}$	isorhamnetin hexoside	−0.31	3
65	3.65	211.97		507.1147	315.0145	$C_{23}H_{24}O_{13}$	syringetin hexoside	0.50	3
66	3.66	199.28		449.0726	316.0222/317.0283, 287.0197, 270.0171	$C_{20}H_{18}O_{12}$	myricetin pentoside	0.07	3
67	3.69	192.21	190	433.0413	300.9986, 299.9914	$C_{19}H_{14}O_{12}$	ellagic acid pentoside	0.21	3
68	3.76	210.06	208.14	447.0944	285.0401	$C_{21}H_{20}O_{11}$	luteolin 7-glucoside	2.53	1
69	3.77	199.56	198.33	463.0884	300.0275, 271.0248, 255.0299, 243.0297	$C_{21}H_{20}O_{12}$	quercetin 3-galactoside	0.32	1
70	3.80	199.70	199.75	463.0884	300.0276, 271.0249, 255.0298, 151.0037	$C_{21}H_{20}O_{12}$	quercetin 3-glucoside	0.49	1
71	3.81	233.29	233.54	609.1462	463.0882, 301.0345, 271.0249, 255.0298	$C_{27}H_{30}O_{16}$	rutin	0.10	1
72	3.83	222.49		599.1045	447.0920, 313.0564, 285.0393, 169.0144	$C_{28}H_{24}O_{15}$	astragalin gallate	0.36	3
73	3.87	197.35		447.0567	314.0072, 299.9910, 160.016	$C_{20}H_{16}O_{12}$	methyl ellagic acid pentoside	−0.49	3
74	3.93	151.08	149.78	300.999	283.9962, 257.0094, 229.0142, 185.0243	$C_{14}H_6O_8$	ellagic acid	−0.01	1
75	4.06	196.78	196.50	433.0774	300.0275, 301.0344, 271.0245, 255.0295	$C_{20}H_{18}O_{11}$	quercetin 3-arabinoside	−0.63	2
76	4.07	228.78		615.0988	463.0875, 433.0772, 301.0344	$C_{28}H_{24}O_{16}$	galloyl-quercetin-hexoside	−0.65	3
77	4.07	200.53	196.20	447.0928	301.0344, 271.0245, 255.0295, 151.0036	$C_{21}H_{20}O_{11}$	quercetin 7-rhamnoside	−1.17	2
78	4.11	163.72	162.78	317.0306	287.0209, 151.0036, 109.0296	$C_{15}H_{10}O_8$	myricetin	0.85	1
79	4.12	197.49		447.056	315.0142, 299.9908, 285.0394, 227.0347	$C_{20}H_{16}O_{12}$	methyl ellagic acid pentoside	−2.03	3
80	4.13	180.92		349.0561	197.0453	$C_{16}H_{14}O_9$	digallic acid ethyl ester	−1.07	3
81	4.14	230.58		593.1505	447.0925, 285.0393, 257.0430	$C_{27}H_{30}O_{15}$	kaempferol-hexoside-rhamnoside	−1.25	3
82	4.16	200.10	199.59	447.0924	284.0323, 256.0344, 227.0347	$C_{21}H_{20}O_{11}$	kaempferol 3-glucoside	−1.91	2
83	4.18	211.84		583.1089	463.0876, 300.0274	$C_{28}H_{24}O_{14}$	quercetin hydroxybenzoyl hexoside	−0.75	3
84	4.2	223.67		585.0888	433.0774	$C_{27}H_{22}O_{15}$	quercetin galloyl-pentoside	0.40	3
85	4.37	161	161.74	301.0347	255.0553	$C_{15}H_{10}O_7$	morin	−2.18	1
86	4.38	195.59		417.0824	285.0399, 255.0299, 227.0349	$C_{20}H_{18}O_{10}$	kaempferol 7-pentoside	−0.65	3
87	4.64	160.68	160.25	301.0354	271.0249, 245.0463, 151.0036	$C_{15}H_{10}O_7$	quercetin	0.07	1
88	5.07	158.65	157.47	285.0405	267.0297, 227.0347	$C_{15}H_{10}O_6$	kaempferol	0.23	1

https://doi.org/10.1021/acs.jafc.1c02845
J. Agric. Food Chem. 2021, 69, 10856−10868

Table 1. continued

[a]Retention time (RT), collision cross section (CCS).

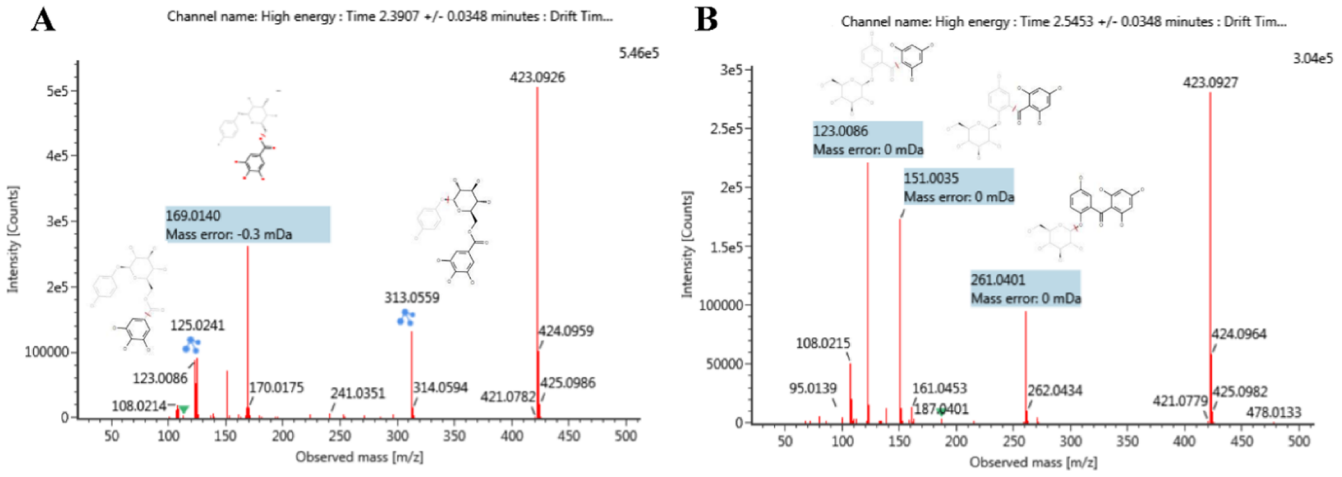

Figure 1. High energy spectrum and fragment assignment of compound **29** (galloyl arbutin) and compound **33** (hypericophenonoside).

when calculating the elemental formula mass error (<5 ppm) and i-Fit confidence, which is a measure of how well the theoretical isotope pattern of a proposed composition matches the measured data. Once an elemental composition for each marker had been derived, searches for compounds with that formula were performed in the ChemSpider database, automatically by UNIFI, and in PubChem manually. Structures of the compounds returned from the database searches were automatically submitted to fragment match, which matched substructures to ions in the high energy data of each marker, providing added confidence in the compound assignment. Additionally, the MS/MS spectral databases METLIN and Massbank of North America (MoNA) were used for the interpretation of some compounds.

A total of 333 CCS values of the deprotonated ion of the phenolic compounds were mined from a range of publications[23−28] and compared to the experimental CCS measured using the Vion IMS-QTof mass spectrometer in our lab (with a ΔCCS% threshold of 2%). For compounds for which a CCS value was not available in the literature, a theoretical CCS value was determined by AllCCS[22] (http://allccs.zhulab.cn/), which was then compared to the measured CCS value. A tolerance of up to 5% between the measured and predicted CCS values was considered to be acceptable.

All the identified compounds were assigned an identification confidence level proposed by Celma et al.[29] and based on the experimental data (RT, CCS value, m/z value, and fragments) acquired during the analysis. The five confidence levels are

- Level 1, empirical data of unknowns fully match that of a reference standard.
- Level 2, an exact structure is proposed but not cross-checked against its respective chemical standard.
- Level 3, different compounds are compatible with empirical data.
- Level 4, only molecular formula can be determined, and no fragmentation information is available.
- Level 5, only exact mass is obtained.

2.6. Quantification of Phenolic Compounds in Bearberry Leaves. Fourteen phenolic compounds were quantified using an external standard calibration, where the standards at different concentrations were injected under the same conditions as the samples by means of a matrix-matched calibration curve. Phenolic compounds always show precursor ion $[2M - H]^-$ when high concentrations are injected, and as such, we used the sum of the responses of $[M - H]^-$ and $[2M - H]^-$ to derive the calibration curve.

The limit of detection (LOD) and limit of quantification (LOQ) of the analytes were calculated by the calibration curve procedure using the slope and standard deviation of regression.

2.7. 2,2-Diphenyl-1-picrylhydrazyl Radical Scavenging Capacity. The IC_{50} values of 14 standards were determined using 2,2-diphenyl-1-picrylhydrazyl (DPPH) assay, for which a series of standard solutions at different concentrations (200−1000 mg/kg for arbutin and 10−200 mg/kg for other standards) were prepared in 70% ethanol (v/v). Exactly 100 μL of each standard solution was mixed with 3.5 mL of the DPPH solution at a concentration of 30 μg/g and placed in the dark at room temperature for 30 min. The absorbance at 515 nm was measured with a UV−vis spectrophotometer (UV-1700, Shimadzu, Japan) using 10 mm quartz cuvettes. A solution of 100 μL of 70% (v/v) ethanol and 3.5 mL of DPPH was used as the control blank. Inhibition percentage was calculated using the following equation

$$I\% = \frac{A_0 - A_s}{A_0} \times 100\%$$

where $I\%$ is the inhibition rate (%), A_0 is the absorbance of the control blank, and A_s is the absorbance of each sample. IC_{50} (mg/kg), the concentration at which 50% of the inhibition rate is obtained, was calculated using calibration curves by plotting $I\%$ versus concentrations.

3. RESULTS AND DISCUSSION

Table 1 shows the 88 phenolic compounds identified in bearberry leaves together with their RT, CCS value, observed m/z, fragment ions, molecular formula, mass error, and confidence level. 14 arbutin derivatives, 33 hydrolyzable tannins, 6 flavanols, 26 flavonols, and 9 other compounds were identified; 17 of these compounds were confirmed using the reference standards. Gallotannins and quercetin glycosides were the dominant compounds detected in the bearberry leaves, while myricetin glycosides gave a low response. Phenolic acids such as coumaric acid, ferulic acid, caffeic acid, and chlorogenic acid were not detected in the bearberry leaves. This has also been shown to be the case in previous studies.[8,30]

The mass error and CCS variation of six of the reference compounds in the Test-Mix are shown in Figure S1. It can be seen that the mass differences throughout this analysis were

https://doi.org/10.1021/acs.jafc.1c02845
J. Agric. Food Chem. 2021, 69, 10856−10868

less than 3 ppm and CCS tolerances were within 2%, thus indicating the precision and stability of the Vion IMS-QTof mass spectrometer.

3.1. Arbutin and Derivatives. Compound **6** was identified as arbutin by comparison with the reference standard. A fragment ion at m/z 109.0284 could be due to the loss of hexoside. The $[M - H]^-$ ion with m/z 423.0928 was detected for compounds **16**, **17**, **21**, and **29**, together with fragment ions at m/z 313.0561 $[M - H - C_6H_6O_2]^-$, 169.0140, and 125.0241. The fragment ion with m/z 313.0561 corresponds to the loss of hydroquinone, and the four compounds can be assigned as galloyl arbutin isomers. The high energy spectrum of compound **29**, together with fragment assignments, is shown in Figure 1A. Compound **23** was identified as picein by suspect screening; picein was targeted because it has been found in bearberry leaves in a previous study.[8] The precursor ion of picein was found to be $[M + HCOO]^-$ with an m/z value of 343.1031. The less abundant $[M - H]^-$ ion was also observed at m/z 297.0976, and a fragment ion at m/z 135.0449 $[M - H - C_6H_{10}O_5]^-$, which corresponds to the loss of the glucosyl group, was detected in the high energy spectrum. The $[M - H]^-$ ion was found for compound **30** with an m/z value of 313.0925, and the compound was identified as 6-*O*-acetylarbutin by suspect screening.[9] The predicted CCS value of this compound was found to be 170.70 Å^2, which perfectly matched the measured CCS value of 168.93 Å^2.

The $[M - H]^-$ ion was observed for compound **33** with an m/z value of 423.0930, which corresponds to the molecular formula of galloyl arbutin; however, the m/z values of the fragment ions detected for the compound were 261.0401 $[M - H - C_6H_{10}O_5]^-$, 151.0035, 123.0086, and 108.0215. In contrast to compounds **16**, **17**, **21**, and **29**, the fragment ion with m/z 169.0142 was not observed in the high energy spectrum (Figure 1B). This indicated that a hexosyl moiety was located on one side of the structure and that the gallic acid group is not present. The compound was tentatively identified as tetrahydroxy-glucopyranosyloxy-benzophenone, among the different structures corresponding to the fragmentation information. Hypericophenonoside contains an arbutin unit in its structure, which was found in *Hypericum annulatum* previously,[31] and its possible fragments are shown in Figure 1B.

The $[M - H]^-$ ion was detected for compound **41** at an m/z value of 447.1506, and this was tentatively assigned as $C_{19}H_{28}O_{12}$. Methyl arbutin has been identified in bearberry leaves in a previous study,[9] and the mass difference between methyl arbutin and this compound is 162.0528 Da, which corresponds to a hexosyl group. Therefore, compound **41** was tentatively identified as glucopyranosyl methyl arbutin. The $[M - H]^-$ ion was observed for compound **45** at an m/z value of 575.1038. Three fragment ions were observed for this compound with m/z values of 465.0670 $[M - H - C_6H_6O_2]^-$, 423.0930 $[M - H - C_7H_4O_4]^-$, and 313.0564 $[M - H - C_6H_6O_2 - C_7H_4O_4]^-$, which correspond to the loss of hydroquinone, the galloyl group, and the two losses combined, respectively. Compounds **48** and **51** have the same m/z value for the $[M - H]^-$ ion as compound **45**, and the three compounds were tentatively identified as digalloyl arbutin isomers.

The $[M - H]^-$ ion was detected for compound **52** at an m/z value of 727.1155. Three fragment ions with m/z values of 575.1048 $[M - H - C_7H_4O_4]^-$, 557.0946 $[M - H - C_7H_6O_5]^-$, and 405.0819 $[M - H - C_7H_4O_4 - C_7H_6O_5]^-$ were also observed, and the compound was identified as trigalloyl arbutin. The $[M - H]^-$ ion was also detected for compound **53** at an m/z of 437.1088, and fragment ions with m/z values of 313.0564, 241.0351, and 168.0062 were also observed. Fragment 241.0351 could result from the loss of gallic acid and a methyl group. 6″-galloyl arbutin and methyl arbutin have previously been detected in bearberry;[9] therefore, compound **53** was inferred as 6″-galloyl methyl arbutin. The predicted CCS value of this compound is 200.50 Å^2, which matched the measured CCS value of 195.91 Å^2 to within the 5% tolerance.

3.2. Hydrolyzable Tannins and Derivatives. *3.2.1. Gallic Acid and Gallotannins.* The $[M - H]^-$ ion was detected for compound **4** with an m/z value of 493.1194, together with fragment ions with m/z values of 323.0988 $[M - H - C_7H_6O_5]^-$, and 161.0457 $[M - H - C_7H_6O_5 - C_6H_{10}O_5]^-$. The compound was tentatively assigned as galloyl di-hexoside. Compound **7** was identified as gallic acid, and this assignment was confirmed using a certified standard.

The $[M - H]^-$ ion, with an m/z value of 331.0667, was detected for compounds **3**, **9**, **10**, and **11** and exhibited a neutral loss of a hexose moiety to yield a fragment ion with an m/z value of 169.0139 $[M - H - C_6H_{10}O_5]^-$. Other common fragment ions for these four species were detected with m/z values of 125.0242, 211.0244, and 271.0456. The spectral data are consistent with that of 1-galloyl glucose, and possible structures for the fragments have been presented in a previous study.[32] These four compounds were tentatively identified as monogalloyl glucose isomers. The variation of the measured CCS values for these four isomers was less than 2%, and there was no available standard to be used for confirmation. The $^{TW}CCS_{N2}$ value of monogalloyl glucose was detected as 168 Å^2,[25] showing a good match with measured CCS values herein (170.53−173.49 Å^2). The position of a galloyl moiety on the hexose could not be inferred from the data because the different positional isomers had very similar arrival time distributions yielding almost identical CCS values.

The $[M - H]^-$ ion was detected for compounds **12** and **18** at an m/z value of 325.0563, together with a fragment ion at an m/z value of 169.0141 $[M - H - C_7H_8O_4]^-$, which corresponds to the neutral loss of a shikimate moiety. Based on these observations, the compounds were tentatively identified as galloylshikimic acid. The predicted CCS value of both 3- and 5-galloylshikimic acid is 169.30 Å^2, which is within 1.8% of the measured CCS value of 172.33 Å^2 for these compounds. The precursor ion for compound **54** was found to have an m/z value of 197.0454. Two fragment ions were also determined for this compound with m/z values of 169.0141 and 124.0163, with the former fragment corresponding to the loss of an ethyl group. The compound was identified as ethyl gallate, and the measured high energy spectrum was found to be consistent with that previously published.[33] The $[M - H]^-$ ion for compound **80** was detected at an m/z value of 349.0561, together with a fragment ion at an m/z value of 197.0453 $[M - H - C_7H_4O_4]^-$, which corresponds to the loss of a galloyl group. The high energy spectrum of this compound was challenging to interpret due to its low ionization efficiency. The compound was tentatively assigned as digallic acid ethyl ester. The $[M - H]^-$ ion for compounds **5**, **13**, **19**, **22**, and **27** was observed with an m/z value of 483.0775. In addition, fragment ions were detected with m/z values of 331.0673, 271.0457, and 211.0246, with the first of these explained by the

https://doi.org/10.1021/acs.jafc.1c02845
J. Agric. Food Chem. 2021, 69, 10856−10868

loss of a galloyl moiety. The 1,6-digalloyl glucose compound was previously isolated and identified in bearberry leaves,[9] and compound **27** showed a higher response than other ions. The identity of compound **27** possibly was 1,6-digalloyl glucose; however, due to the lack of the reference standard, this identification was not confirmed. The $^{TW}CCS_{N2}$ value of digalloyl glucose was detected as 191 Å^2,[25] which matched well with the measured CCS values 192.89−194.11 Å^2.

The $[M - H]^-$ ion for compounds **20**, **24**, **26**, and **38** was detected at an m/z value of 635.0884, together with fragment ions at m/z values 465.0669 $[M - H - C_7H_6O_5]^-$ and 313.0562 $[M - H - C_7H_6O_5 - C_7H_4O_4]^-$, which correspond to the loss of gallic acid and a galloyl group, respectively. Fragments at m/z 169.0141 and 125.0242 also indicated the presence of gallic acid. These four compounds were identified as trigalloyl glucose. Compound **38** showed a higher response, which can be 3,4,6-trigalloylglucose or 1,3,6-trigalloylglucose, because these two compounds were previously isolated in bearberry leaves,[9,10] but the reference standards were required for this identification.

The $[M - H]^-$ ion for compound **47** was detected at an m/z value of 787.1003, together with fragment ions at m/z values 635.0891 $[M - H - C_7H_4O_4]^-$, 617.0782 $[M - H - C_7H_6O_5]^-$, 465.0670 $[M - H - C_7H_6O_5 - C_7H_4O_4]^-$, and 447.0568 $[M - H - 2C_7H_6O_5]^-$. This compound was tentatively assigned as tetragalloyl glucose. The $[M - H]^-$ ions for compounds **37** and **56** had an m/z value of 787.0997, which was very similar to the m/z value of compound **47**; these two compounds were therefore assigned as tetragalloyl glucose isomers. The $^{TW}CCS_{N2}$ value of tetragalloyl glucose was detected as 264 Å^2,[25] which matched well with the CCS values 266.49−270.27 Å^2 herein. The $[M - H]^-$ ion for compound **57** was detected with an m/z value of 939.1108 and was confirmed as 1,2,3,4,6-pentagalloyl glucose using a reference standard.

3.2.2. Ellagic Acid and Ellagitannins. The $[M - H]^-$ ion for compound **32** was detected at an m/z value of 951.0745, together with two major fragment ions with m/z values of 933.0650 and 300.9988, consistent with the fragments of geraniin.[34] The presence of a hexahydroxydiphenyl (HHDP) group was also confirmed by the observation of the characteristic fragment ion with an m/z value of 300.9988. Therefore, this compound was identified as geraniin isomer. The $[M - H]^-$ ion for compound **39** was observed with an m/z value of 633.0734. This compound also exhibited the loss of 170 Da (gallic acid) and 162 Da (hexoside), producing two fragment ions at m/z 463.0513 and 300.9989, respectively, in the high energy spectrum. The data match well with that for corilagin presented in a previous publication.[35] Besides, corilagin was previously isolated in bearberry leaves,[9] and compound **39** was tentatively assigned as corilagin. The CCS value of corilagin was not found in the literature; however, a $^{TW}CCS_{N2}$ value of 222 Å^2 of galloyl−HHDP−glucose was detected in a previous study,[25] which matched well with the measured value of 221.94 Å^2.

Compounds **46** and **62** show $[M - H]^-$ ions with m/z values of 965.0908 and 955.1064, respectively. The ionization efficiency of these two compounds was low, though, and no fragments of these two compounds were detected in the high energy spectrum. By searching their formulas in PubChem, many compounds containing units of ellagic acid were found. As such, these two compounds were only tentatively assigned as ellagitannins, and no more specific annotations were given.

The $[M - H]^-$ ion for compound **67** was detected with an m/z value of 433.0413. An associated fragment ion with an m/z value of 300.9986 $[M - H - C_5H_8O_4]^-$ indicated the presence of ellagic acid, with the reduction in mass by 132.0428 Da, which corresponds to the loss of pentoside. The compound was identified as ellagic acid pentoside, with an experimental $^{TW}CCS_{N2}$ value[25] of 190 Å^2 within 2% of the measured value of CCS 192.21 Å^2. Compound **60** was also tentatively assigned as ellagic acid pentoside because the m/z value of the $[M - H]^-$ ion for this compound was measured as 433.0409. Compound **74** was identified as ellagic acid by the reference standard. The $[M - H]^-$ ions of compounds **73** and **79** were both detected with an m/z value of 447.0560. Fragment ions with m/z values of 315.0142 $[M - H - C_5H_8O_4]^-$ and 299.9908 $[M - H - C_5H_8O_4 - CH_3]^-$ were detected in the high energy spectra with the mass reductions of 132.0417 and 15.0234 Da, indicating the loss of pentoside and a methyl group, respectively. The two compounds were tentatively identified as methyl ellagic acid pentoside isomers.

3.3. Flavanols. The $[M - H]^-$ ions for compounds **28**, **36**, **43**, and **50** were identified as (+)-catechin, (−)-epigallocatechin gallate, (−)-epicatechin, and (−)-epicatechin 3-gallate, respectively, by comparing with reference standards. The $[M - H]^-$ ions for compounds **34** and **40** were detected with m/z values of 729.1457 and 881.1571, respectively, with the mass difference of 152.0144 between these values corresponding to a galloyl group. The former compound had fragments with m/z values of 407.0773 and 289.0717 and was assigned as procyanidin gallate. The latter compound had fragment ions with m/z values of 729.1438, 711.1346, 559.1251, 541.1155, 407.0774, and 289.0716 and was tentatively identified as procyanidin di-gallate.

3.4. Flavonols. The majority of flavonols exist naturally as glycosides. The aglycones and glycosyl groups and their relative position on the scaffold can affect the RT of flavonoid glycosides. The general elution order of the aglycones was myricetin, quercetin, followed by kaempferol; while the elution order of the glycosyl group was di-*O*-glycoside, O-galactoside, *O*-glucoside, *O*-rutinoside, *O*-neohesperidoside, with *O*-rhamnoside the last to elute. As for the influence of the sugar position, *C*-glycosides elute before *O*-glycosides and the elution order observed was 8-*C*-, 6-*C*-, 3′,7-di-*O*-, 7-*O*-, 4′-*O*-, and finally 3-*O*-.[36] The masses of the following glycosyl groups were also repeatedly observed: hexoside ($C_6H_{10}O_5$, m/z 162.0528), pentoside ($C_5H_8O_4$, m/z 132.0423), rhamnoside ($C_6H_{10}O_4$, m/z 146.0579), and glucuronide ($C_6H_8O_6$, m/z 176.0473).

The $[M - H]^-$ ion for compound **59** was detected with an m/z value of 493.0622, and associated fragment ions with m/z values of 315.0150, 151.0401, and 137.0245 were observed in the associated high energy data. This compound was tentatively assigned as myricetin glucuronide. The $[M - H]^-$ ion was detected for compounds **35** and **42** with an m/z value of 447.0667; however, the high-energy spectrum was difficult to interpret due to the presence of coeluting compounds, and the only fragment ion that could be reliably assigned was that with an m/z value of 271.0459 for compound **35**. In this case, the structures of the two isomers were too similar to separate using ion mobility. Because compound **59** had been identified as myricetin glucuronide, and taking into consideration the elution order discussed above, together with the mass spectral data, these two compounds were both tentatively assigned as isomers of quercetin glucuronide. An experimental $^{TW}CCS_{N2}$

https://doi.org/10.1021/acs.jafc.1c02845
J. Agric. Food Chem. 2021, 69, 10856−10868

value (193.70 Å^2) of quercetin 3-glucuronide was reported previously,[23] which is similar to the measured CCS value (around 195.50 Å^2) of compounds **35** and **42**.

The $[M - H]^-$ ion for compound **58** was observed with an m/z value 465.1035, together with fragment ions with m/z values 313.0952, 303.0514, 285.0414, and 151.0414 in the high energy data. These spectral data were in agreement with that of taxifolin 3-glucoside in MoNA. The identification was further confirmed by the comparison of the measured CCS value of 195.32 Å^2 for this compound with that of the predicted value of 196.70 Å^2. The $[M - H]^-$ ion detected for compound **61** had an m/z value of 479.0833, and three fragment ions, typical of myricetin, were observed in the high energy data with m/z values of 316.0226, 287.0197, and 271.0248. The fragment with m/z 316.0226 is consistent with the mass of a radical myricetin anion, which can be produced by the loss of a hexosyl group through homolytic cleavage. This compound was identified as myricetin hexoside.

The $[M - H]^-$ ion for compound **63** was detected with an m/z value of 615.0991, together with fragment ions with m/z values of 463.0879 $[M - H - C_7H_4O_4]^-$, 313.0565 $[M - H - 301]^-$, 301.0346 $[M - H - C_7H_4O_4 - C_6H_{10}O_5]^-$, and 169.0142 [gallic acid $- H]^-$. The fragments and mass differences indicated the presence of quercetin aglycone, a hexosyl group, and a galloyl group in the core structure. Based on these observations, the compound was assigned as galloyl-quercetin-hexoside. The observed $[M - H]^-$ ion for compound **76** also had an m/z value of 615.0988 but a CCS value of 228.78 Å^2. It is tentatively suggested that this compound may be an isomer of galloyl-quercetin-hexoside. The $[M - H]^-$ ion for compound **64** was detected with an m/z value of 477.103, together with one fragment ion with an m/z value of 299.0200. This compound was tentatively assigned as isorhamnetin hexoside. The $[M - H]^-$ ion for compound **65** was observed with an m/z value of 507.1147 and a CCS measurement of 211.97 Å^2. A fragment ion with an m/z value of 315.0145 was also observed in the high energy data. The compound was tentatively assigned as syringetin hexoside. The $[M - H]^-$ ion for compound **66** was detected with an m/z value of 449.0726 and a CCS value of CCS 199.28 Å^2, together with four fragment ions, typical of myricetin, at m/z values 316.0222, 317.0283 $[M - H - C_5H_8O_4]^-$, 287.0197, and 270.0171. This compound was identified as myricetin pentoside. The $[M - H]^-$ ion for compound **68** was observed with an m/z value of 447.0944, together with a fragment ion at an m/z value of 285.0401. This compound was identified as luteolin 7-glucoside by a reference standard.

Compounds **69**, **70,** and **71** were identified as quercetin 3-galactoside, quercetin 3-glucoside, and rutin, respectively, by comparing with reference standards. The $[M - H]^-$ ion for compound **72** was detected with an m/z value of 599.1045 and a CCS value of 222.49 Å^2. Four fragment ions with m/z values of 447.0920 $[M - H - C_7H_4O_4]^-$, 313.0564 [$M - H$ − kaempferol aglycone], 285.0393 $[M - H - C_7H_4O_4 - C_6H_{10}O_5]^-$, and 169.0144 were observed in the high energy data. The measurements were consistent with astragalin gallate. The predicted CCS values of astragalin 2″-gallate and astragalin 6″-gallate are 220.60 and 220.20 Å^2, respectively, both within 1.1% of the measured value; therefore, the position of gallate on the structure cannot be deduced from the current data. The $[M - H]^-$ ion for compound **75** was observed with an m/z value of 433.0774, together with fragment ions with m/z values 300.0275, 271.0245, 255.0295, and 151.0036 in the high energy data. The fragment with an m/z value of 300.0275 was associated with the loss of pentoside, while the lower mass fragments are typical of quercetin. Because avicularin (quercetin 3-arabinoside) has previously been detected in bearberry leaves,[9] the compound was assigned as quercetin 3-arabinoside, which has a predicted CCS value of 196.50 Å^2, consistent with the measured value of 196.78 Å^2 herein.

The $[M - H]^-$ ion for compound **77** was observed with an m/z value of 447.0928. The high energy spectrum of this compound is shown in Figure 2. The most abundant fragment

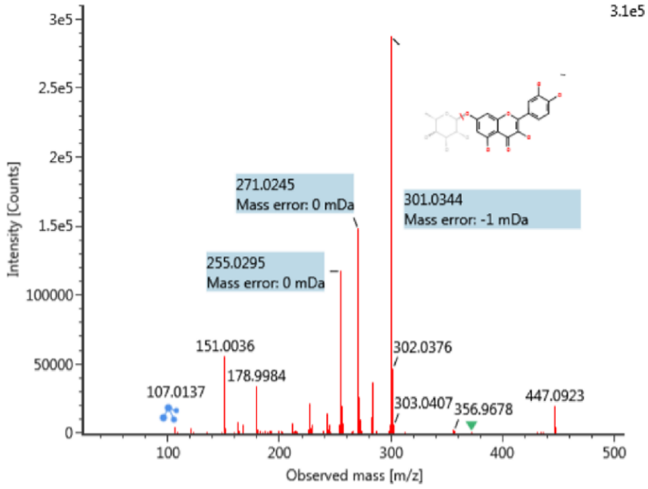

Figure 2. High energy spectrum of compound **77**, quercetin 7-rhamnoside, $[M - H]^-$ m/z 447.0923.

ion has an m/z value of 301.0344 $[M - H - C_6H_{10}O_4]^-$, which corresponds to the loss of rhamnoside. Additional fragments are observed with m/z values 271.0245, 255.0295, and 151.0036, which are typical of quercetin aglycone. As such, the compound was initially identified as quercetin rhamnoside. A certified standard of quercetin 3-rhamnoside was injected to confirm the identification; however, the most abundant fragment ion observed for the standard had an m/z value of 300.0272, which corresponds to the radical quercetin aglycone. The glycosylation position can affect the relative abundance of radical aglycone to the aglycone and 3-*O*-glycoside can facilitate the formation of radical aglycone.[37] The high energy spectrum of compound **77** was subsequently compared to the MS/MS spectrum of quercetin 7-rhamnoside in MoNA with a high degree of correspondence between the two spectra obtained. Additionally, a deviation of 2.8% was observed between the measured CCS values of compound **77** (200.53 Å^2) and quercetin 3-rhamnoside (194.98 Å^2). Based on the fact that all the compounds identified at level 1 showed <2% CCS deviations with reference standards, compound **77** was not assigned as quercetin 3-rhamonoside. Generally, a sugar moiety at the 7-O position would lead to a more extended structure compared to the same sugar moiety at the 3-O position of flavonols. For example, kaempferol 7-glucoside showed a higher experimental CCS value than kaempferol 3-glucoside (208.30 vs 199.59 Å^2).[27] Taking all this information together, compound **77** was identified as quercetin 7-rhamnoside.

Compounds **78**, **85**, **87,** and **88** were identified as myricetin, morin, quercetin, and kaempferol, respectively, by comparing the RT, accurate mass, and CCS values with those obtained from certified standards. The $[M - H]^-$ ion for compound **81** was observed with an m/z value of 593.1505, together with

https://doi.org/10.1021/acs.jafc.1c02845
J. Agric. Food Chem. 2021, 69, 10856−10868

fragment ions with m/z values of 447.0925 $[M - H - C_6H_{10}O_4]^-$, 285.0393 $[M - H - C_6H_{10}O_4\text{-}C_6H_{10}O_5]^-$, and 257.0430 in the high energy data. The fragmentation information indicated the presence of kaempferol aglycone, rhamnoside, and hexoside in the structure. Based on these observations, the compound could be kaempferol-hexoside-rhamnoside. The measured $^{TW}CCS_{N2}$ value of 227.65 Å^2 of kaempferol 7-neohesperidoside was found in a public CCS database,[28] which showed 1.3% deviation with the CCS value of compound **81** (230.58 Å^2). However, the measurement of a reference standard would be required to confirm this identification.

The $[M - H]^-$ ion for compound **82** was observed with an m/z value of 447.0924, together with fragment ions with m/z values of 284.0323, 256.0344, and 227.0347 in the high energy data. The high energy spectrum matched well with the spectrum of kaempferol 3-glucoside in MoNA. In addition, the experimental $^{TIMS}CCS_{N2}$ values of 199.59 Å^2 and 208.30 Å^2 were found for kaempferol 3-glucoside and kaempferol 7-glucoside, respectively, in the literature;[27] the former value was very close to the measured CCS value of 200.10 Å^2 of compound **82**. Hence, the compound was identified as kaempferol 3-glucoside with a relatively high confidence level of 2. The $[M - H]^-$ ion for compound **83** was detected with an m/z value of 583.1089, together with fragment ions at m/z values 463.0876 $[M - H - 120]^-$ and 300.0274. The reduction in mass by 120.0213 Da to yield the larger fragment corresponds to the loss of a hydroxybenzoyl group. The compound was tentatively assigned as quercetin hydroxybenzoyl hexoside. The $[M - H]^-$ ion for compound **84** was observed with an m/z value of 585.088, together with one fragment ion with an m/z value of 433.0774 $[M - H - C_7H_4O_4]^-$, which corresponds to the loss of a galloyl group. The compound was tentatively assigned as quercetin galloyl-pentoside. The $[M - H]^-$ ion of compound **86** was detected with an m/z value of 417.0824. Fragment ions with m/z values of 284.0325 and 285.0399 correspond to the loss of pentoside. Additionally, fragments with m/z values of 255.0299 and 227.0349 indicated the presence of kaempferol, and therefore, this compound was initially assigned as kaempferol pentoside. The response of 285.0399 (Y_0^-) in high energy data was higher than that of 284.0325 {radical kaempferol $[Y_0 - H]^{-\bullet}$}, indicating that pentoside is likely to be at the 7-*O* position of kaempferol. In addition, the predicted CCS values of kaempferol 3-arabinoside and kaempferol 7-arabinoside are 189.30 and 194.00 Å^2, respectively. The latter value was closer to the measured CCS value of 195.59 Å^2 for this compound. Based on these observations, the compound was tentatively identified as kaempferol 7-pentoside. The specific type of glycosyl group cannot be proposed based on current data.

3.5. Organic Acids and Saccharide Derivatives. The $[M - H]^-$ ion for compound **1** was detected with an m/z value of 191.0562 and was identified as quinic acid by the reference standard. The identities of compounds **2**, **8**, **14**, **15**, **31**, **44**, **49**, and **55** were not confirmed due to their limited fragmentation information; however, by searching their formula in PubChem, many candidates belonging to saccharide derivatives were found. For example, the $[M - H]^-$ ion for compound **15** was detected with an m/z value of 315.0718. Two fragment ions were also observed with m/z values of 152.0113 and 108.0216, which correspond to the loss of hexoside and CO_2. Compound **44** was observed with the $[M - H]^-$ ion at m/z 323.1346, from which the elemental composition $C_{13}H_{24}O_9$ was determined, and many saccharide derivatives with different types of sugar moieties were found in PubChem, corresponding to this formula. The identification of these kinds of compounds may need standards or IMS with higher resolving power.[38,39]

3.6. Quantification and Antioxidant Properties of Phenolic Compounds. The equation of the calibration line, the associate coefficient of determination (R^2), linear range, LOD, and LOQ for 14 compounds are shown in Table S3. With the exception of quinic acid, gallic acid, and quercetin 3-glucoside, the coefficients of determination were higher than 0.999, indicating good linearity of the calibration curves. The inclusion of the response of the $[2M - H]^-$ adducts further improved the linearity of the calibration data. For example, in the case of quercetin 3-glucoside, the $[2M - H]^-/[M - H]^-$ ratios at concentrations of 0.2, 0.5, 1, 2, and 5 mg/kg were 0.8, 1.8, 3.2, 5.1, and 8.4%, respectively, and the coefficient of determination increased from 0.9866 to 0.9911 upon considering the response of $[2M - H]^-$. Similar improvements in R^2 were also observed for (−)-epicatechin 3-gallate, (+)-catechin, and quercetin.

The concentrations of the 14 calibrated compounds in bearberry leaves are shown in Table 2. The most abundant compound was arbutin, with a concentration higher than 5% (w/w) on average and even higher than 10% in the samples collected at Chelva, Pina, and Albarracín (Spain). This observation is consistent with that reported in a previous study.[8] Arbutin is the most important antioxidant and antibacterial compound in bearberry leaves, and it can suppress the biosynthesis of melanin in human skin and so is widely used in skin-lightening agents.[40] Another compound showing a relatively high content in bearberry leaves is 1,2,3,4,6-pentagalloglucose, with concentrations ranging from 6.61 to 12.89 mg/g dry weight. Furthermore, quercetin 3-galactoside/quercetin 3-glucoside, quinic acid, and ellagic acid showed concentrations in the ranges 2.72−5.69, 1.41−9.38, and 1.27−8.46 mg/g dry weight, respectively. Compounds such as quercetin 3-galactoside/quercetin 3-glucoside have been reported to play an important role in the antioxidant properties of bearberry leaves.[41] (+)-catechin and (−)-epicatechin 3-gallate showed concentrations of 125−624 and 152−385 mg/kg dry weight, respectively. Flavonols, such as morin and kaempferol, showed concentrations less than 5 mg/kg dry weight.

The antioxidant contribution of the detected compounds in bearberry leaves is related to their concentrations and antioxidant capacity. Therefore, the antioxidant activities of the 14 compounds were determined. Quinic acid did not show a scavenging effect on the DPPH radical even at a concentration of 10 g/kg. The IC_{50} values of the other 13 compounds in the DPPH assay are shown in Figure 3. It can be seen that gallic acid, ellagic acid, (−)-epicatechin 3-gallate, (−)-epigallocatechin 3-gallate, quercetin, and 1,2,3,4,6-pentagalloglucose showed relatively high antioxidant capacity, with IC_{50} values below 100 mg/kg. (+)-Catechin, (−)-epicatechin, morin, and kaempferol showed IC_{50} values in the range of 100−200 mg/kg, while the scavenging effect of arbutin on the DPPH radical was found to be relatively weak (IC_{50} 1694 mg/kg).

The antioxidant contribution of the compounds was defined as the ratio between the concentration in leaves and IC_{50}, both expressed as mg/kg (as shown in Table S4). 1,2,3,4,6-Pentagalloglucose was found to be the highest contributor to

https://doi.org/10.1021/acs.jafc.1c02845
J. Agric. Food Chem. 2021, 69, 10856−10868

Table 2. Concentrations of 14 Compounds in 9 Bearberry Leaves[a]

compounds	bearberry 1	bearberry 2	bearberry 3	bearberry 4	bearberry 5	bearberry 6	bearberry 7	bearberry 8	bearberry 9
quinic acid[2]	2.30 ± 0.31^{ab}	2.04 ± 0.34^{ab}	3.36 ± 0.40^{ab}	1.41 ± 0.16^{a}	5.35 ± 0.76^{b}	2.73 ± 0.19^{ab}	2.79 ± 0.83^{ab}	5.78 ± 0.77^{b}	9.38 ± 0.84^{c}
gallic acid[2]	0.61 ± 0.09^{a}	0.92 ± 0.05^{ab}	1.51 ± 0.11^{abc}	1.67 ± 0.14^{bc}	1.78 ± 0.24^{bc}	2.14 ± 0.18^{c}	5.32 ± 0.70^{f}	3.28 ± 0.43^{d}	2.32 ± 0.12^{c}
ellagic acid[2]	1.27 ± 0.16^{a}	1.29 ± 0.24^{a}	1.76 ± 0.28^{a}	1.29 ± 0.14^{a}	5.21 ± 0.94^{b}	2.35 ± 0.30^{a}	8.46 ± 0.59^{d}	6.85 ± 0.22^{c}	6.02 ± 0.13^{bc}
arbutin[2]	53.92 ± 7.19^{a}	47.29 ± 6.26^{a}	67.57 ± 7.45^{a}	71.87 ± 5.89^{a}	101.62 ± 2.63^{b}	65.90 ± 3.17^{a}	97.90 ± 5.22^{b}	102.43 ± 9.71^{b}	107.04 ± 5.48^{b}
(+)-catechin[1]	130.93 ± 10.99^{a}	299.85 ± 9.62^{b}	278.16 ± 27.45^{b}	460.20 ± 28.75^{c}	125.11 ± 12.91^{a}	586.01 ± 34.63^{d}	624.45 ± 76.48^{d}	315.98 ± 8.06^{b}	260.22 ± 14.43^{b}
(−)-epicatechin1	5.47 ± 0.34^{a}	5.75 ± 0.29^{a}	8.86 ± 0.62^{b}	8.94 ± 1.13^{b}	6.69 ± 0.92^{a}	6.30 ± 0.45^{a}	12.24 ± 0.72^{c}	8.84 ± 0.74^{b}	9.09 ± 0.34^{b}
(−)-epicatechin 3-gallate[1]	152.26 ± 14.99^{a}	357.54 ± 43.56^{de}	309.27 ± 23.21^{bcd}	317.62 ± 21.79^{cde}	259.62 ± 17.02^{bc}	239.58 ± 24.01^{b}	341.82 ± 31.71^{de}	288.36 ± 4.83^{bcd}	384.77 ± 20.81^{e}
(−)-epigallocatechin 3-gallate[1]	13.99 ± 0.39^{a}	28.45 ± 1.71^{bc}	32.37 ± 0.95^{bc}	52.41 ± 3.26^{d}	26.58 ± 1.18^{b}	62.34 ± 7.90^{e}	24.86 ± 1.82^{b}	23.39 ± 1.98^{b}	36.03 ± 3.07^{c}
morin[1]	1.62 ± 0.12^{a}	1.58 ± 0.06^{a}	2.14 ± 0.13^{b}	2.08 ± 0.07^{b}	2.49 ± 0.19^{bc}	2.65 ± 0.34^{c}	nd	nd	nd
kaempferol[1]	1.01 ± 0.06^{a}	1.08 ± 0.08^{a}	1.82 ± 0.14^{bc}	1.47 ± 0.07^{ab}	1.68 ± 0.24^{ab}	3.54 ± 0.35^{d}	5.33 ± 0.48^{f}	2.45 ± 0.28^{c}	4.43 ± 0.25^{e}
quercetin[1]	27.21 ± 1.89^{a}	30.66 ± 3.53^{a}	48.42 ± 4.52^{a}	36.70 ± 1.71^{a}	50.01 ± 5.30^{ab}	88.02 ± 6.39^{bc}	165.63 ± 19.34^{d}	105.86 ± 8.51^{c}	146.49 ± 5.09^{d}
quercetin 3-glucoside[2]	2.72 ± 0.19^{a}	2.79 ± 0.24^{a}	3.23 ± 0.26^{a}	3.20 ± 0.13^{a}	5.13 ± 0.40^{b}	5.18 ± 0.28^{b}	5.52 ± 0.14^{b}	5.20 ± 0.08^{b}	5.69 ± 0.14^{b}
rutin[1]	51.24 ± 2.83^{a}	67.59 ± 6.22^{b}	63.65 ± 3.37^{ab}	51.26 ± 0.76^{a}	64.22 ± 0.22^{ab}	142.57 ± 9.76^{c}	251.04 ± 5.01^{d}	152.28 ± 1.70^{c}	56.02 ± 2.99^{ab}
1,2,3,4,6-pentagalloglucose[2]	7.23 ± 0.45^{ab}	8.28 ± 0.66^{bc}	9.63 ± 0.69^{cd}	6.66 ± 0.42^{a}	10.89 ± 0.78^{de}	6.61 ± 0.71^{a}	12.04 ± 0.31^{ef}	12.89 ± 0.10^{f}	12.75 ± 0.30^{f}

[a](1) mg/kg dry leaves, (2) mg/g dry leaves, nd = not detectable. a, b, c, d, e, and f: mean values with different letters are significantly different within a row.

Figure 3. IC_{50} values of 13 standards in DPPH assay.

the total antioxidant capacity of bearberry leaves due to its high concentration and low IC_{50} value. Although arbutin exhibited a weak scavenging effect on the DPPH radical, this compound presented a relatively high antioxidant contribution due to its high concentration in bearberry leaves. Other compounds with antioxidant contributions that were higher than 10 were gallic acid, ellagic acid, and quercetin 3-glucoside. One important point to highlight is that DPPH scavenging assay is based on the electron donation of antioxidants to DPPH radicals; this assay may not fully mimic the radical scavenging capacity of antioxidants in the read food system due to the existence of other types of free radicals.[42]

3.7. Advantages and Limitations of IMS-HRMS in the Identification of Phenolics. IMS-QTof has proved to be a powerful tool for the analysis of small molecules.[29,43−45] The relatively high mass resolving power coupled to an ion mobility separation dimension increases peak capacity and can separate coeluting compounds. This is demonstrated in Figure 4, which should make clear the separation of the coeluting compounds quercetin 3-glucoside and rutin. Data-independent acquisition (DIA) is a commonly used mass spectrometry acquisition technique, in which all ions within a selected m/z range are acquired and fragmented. Accurate assignment of product ions to the respective precursor ions can be challenging because fragment ions could originate from multiple coeluting precursor ions. Arrival time alignment facilitated by IMS eliminates many of the interfering ions, resulting in cleaner high energy spectra, thus facilitating the spectral interpretation without compromising the speed of acquisition. In addition to the arrival time alignment, CCS provided by IMS also increases the confidence of identification.

Despite these advantages, some limitations still exist. Coeluting analytes cannot be separated if their arrival times are close to each other (similar mobility constant, K). This has been demonstrated here for quercetin 3-galactoside and quercetin 3-glucoside were not separated by IMS. In fact, in this study, the precursor and fragment ions were considered to be related if the difference in their arrival times was less than 0.23 ms. For example, quercetin 3-arabinoside {$[M - H]^-$ m/z 433.0774} and quercetin 7-rhamnoside {$[M - H]^-$ m/z 447.0928} were detected with arrival times of 5.63 and 5.77 ms, respectively, and their RTs were almost identical at 4.06

https://doi.org/10.1021/acs.jafc.1c02845
J. Agric. Food Chem. 2021, 69, 10856−10868

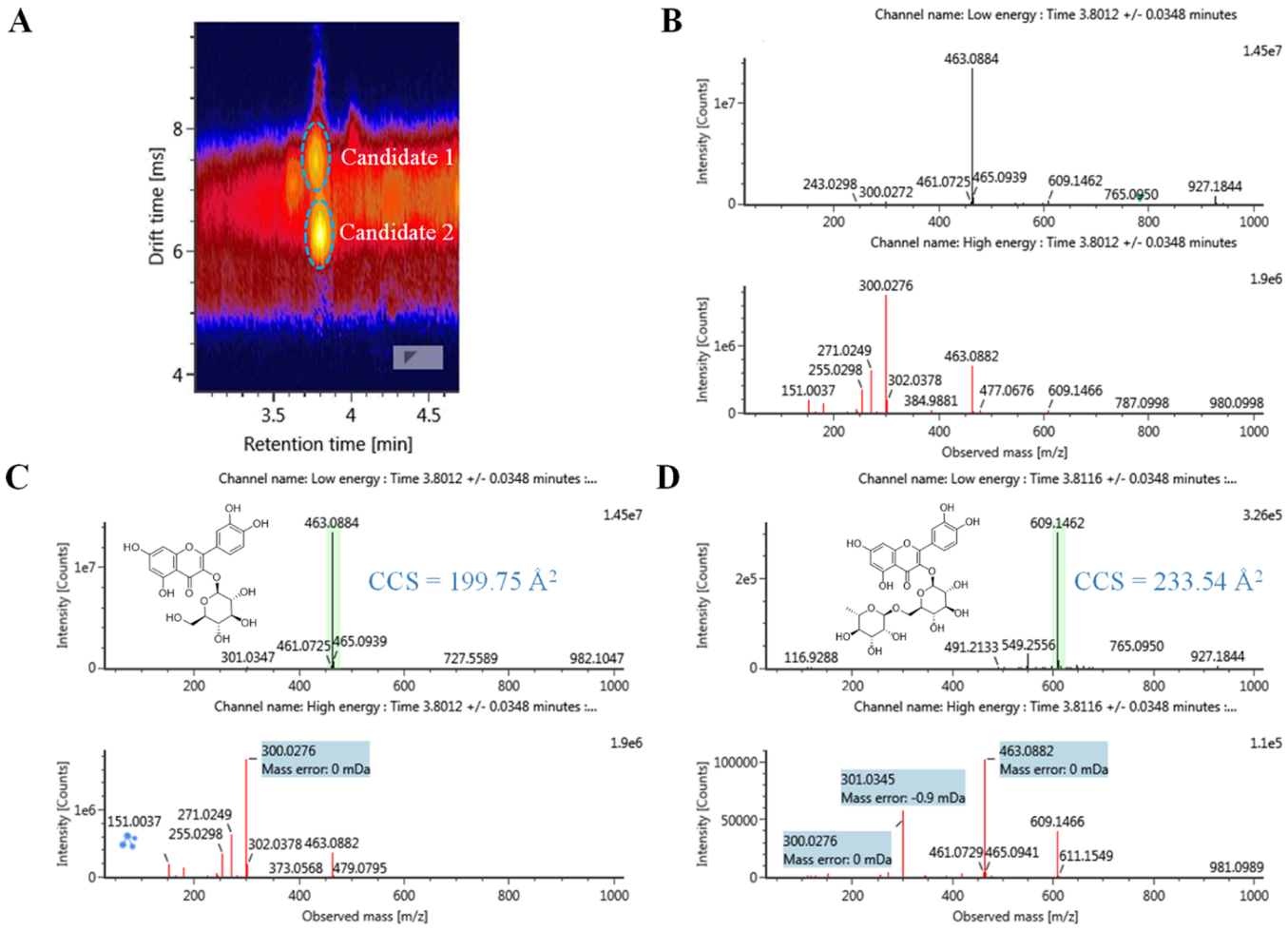

Figure 4. Two components coeluting at RT 3.8 min (A), low and high energy mass spectra at RT 3.81 min (B), and clean mass spectra of quercetin 3-glucoside (C) and rutin (D) produced by arrival time alignment (resolved by IMS).

and 4.07 min, respectively. The precursor ions for both compounds appear in the low energy spectrum even after the arrival time alignment, as shown in Figure S2, and as such, fragment assignment becomes challenging, especially if the two compounds share certain fragments. In order to separate these compounds by IMS, higher resolution in the ion mobility dimension is needed.

An additional limitation for the confident use of CCS values, produced by IMS-QTof experiments for untargeted screening, is the lack of published empirical CCS values; it will be much easier and more reliable for the identification of compound 77 if there is an experimental CCS value available for quercetin 7-rhamnoside. As a matter of fact, many experimental CCS values of flavonols are unavailable due to the high price of commercial standards, such as quercetin 3-glucuronide and myricetin 3-glucuronide. In most cases, the distinction of isomers is based solely on predictive CCS values obtained from machine learning algorithms. Although current errors in the predicted CCS values are within 5% for many compounds, this is still a margin of error that is too large to make a confident identification. As an example from this work, three tetragalloyl glucose isomers were detected; however, CCS predictions were not sufficient to assign the position of the glycosyl moiety on the scaffold. Finally, although deviations of empirical CCS values from different TWIMS systems, and between different laboratories, have been shown to be less than 2%,[21,29,46] stereoisomers can have CCS values that are within 2% of each other. For example, (+)-catechin and (−)-epicatechin have CCS values of 156.61 and 156.54 Å^2, respectively, and would require IMS resolving power capable of differentiating CCS values within 0.05% to separate them. Thus, the identification of challenging isomers still requires higher precision in the empirical CCS values in addition to greater IMS resolution.

In conclusion, IMS-QTof was proved to be a powerful tool for the characterization of phenolic compounds. Some structural isomers, such as quercetin 7-rhamnoside and quercetin 3-rhamnoside, can be identified based on their different CCS values, and the addition of ion mobility dimension makes the mass spectra clearer and more interpretable. Higher resolution of IMS and more empirical CCS values are needed to support the application of IMS in phenolic compound characterization.

■ ASSOCIATED CONTENT

Supporting Information

The Supporting Information is available free of charge at https://pubs.acs.org/doi/10.1021/acs.jafc.1c02845.

Calibration substances and their CCS values; negative ion measurements for the compounds in the Test-Mix solution; calibration data for 14 standards; antioxidant contribution of 13 standards in 9 bearberry leaves (n = 3); analytical sequence of *Arctostaphylos uva-ursi* leaf

https://doi.org/10.1021/acs.jafc.1c02845
J. Agric. Food Chem. 2021, 69, 10856−10868

samples; mass errors and CCS percentage deviations of six compounds in the Test-Mix solution measured throughout the analysis; and low energy and high energy spectrum of compound **75**, quercetin 3-arabinoside, $[M - H]^-$ m/z 433.0774 and compound 77, quercetin 7-rhamnoside, $[M - H]^-$ m/z 447.0928 (PDF)

CCS of 333 phenolic compounds (XLSX)

AUTHOR INFORMATION

Corresponding Author

Cristina Nerin − *Department of Analytical Chemistry, Aragon Institute of Engineering Research I3A, CPS-University of Zaragoza, 50018 Zaragoza, Spain;* orcid.org/0000-0003-2685-5739; Phone: +34 976761873; Email: cnerin@unizar.es

Authors

Xue-Chao Song − *Department of Analytical Chemistry, Aragon Institute of Engineering Research I3A, CPS-University of Zaragoza, 50018 Zaragoza, Spain*

Elena Canellas − *Department of Analytical Chemistry, Aragon Institute of Engineering Research I3A, CPS-University of Zaragoza, 50018 Zaragoza, Spain*

Nicola Dreolin − *Waters Corporation, SK9 4AX Wilmslow, U.K.*

Jeff Goshawk − *Waters Corporation, SK9 4AX Wilmslow, U.K.*

Complete contact information is available at: https://pubs.acs.org/10.1021/acs.jafc.1c02845

Author Contributions

X.-C.S.: conceptualization, methodology, software, investigation, and writing—original draft. E.C.: supervision, conceptualization, and writing—review and editing. C.N.: supervision, funding acquisition, and writing—review and editing. N.D.: software, equipment, review, and editing. J.G.: software, equipment, review, and editing.

Notes

The authors declare no competing financial interest.

ACKNOWLEDGMENTS

X.-C.S. acknowledges the grant received from the China Scholarship Council (201806780031). The authors thank Esther Asensio from the Department of Analytical Chemistry, University of Zaragoza, and Ester Sales from the Department of Agricultural Sciences and the Natural Environment, Plant Production Area, Escuela Politécnica Superior de Huesca, University of Zaragoza, for sampling the bearberry specimens and providing the quercetin 3-glucoside, myricetin, and myricitrin standards. The authors acknowledge the Project RTI2018-097805-B-I00.

ABBREVIATIONS

CCS, collision cross section; RT, retention time,; UPLC-IMS-QTof, ultrahigh performance liquid chromatography coupled to ion mobility spectroscopy and a quadrupole-time-of-flight mass spectrometer; CID, collision-induced dissociation; DTIMS, drift tube ion mobility spectrometry; TWIMS, traveling wave ion mobility spectrometry; ESI, electrospray ionization; BPI, base peak intensity; MoNA, Massbank of North America; LOD, limit of detection; LOQ, limit of quantification; S/N, signal-to-noise ratio; R^2, determination coefficient; DIA, data-independent acquisition

REFERENCES

(1) Naczk, M.; Pegg, R. B.; Amarowicz, R. Protein-precipitating capacity of bearberry-leaf (Arctostaphylos uva-ursi L. Sprengel) polyphenolics. *Food Chem.* **2011**, *124*, 1507−1513.

(2) Mazza, G.; Fukumoto, L.; Delaquis, P.; Girard, B.; Ewert, B. Anthocyanins, phenolics, and color of Cabernet Franc, Merlot, and Pinot Noir wines from British Columbia. *J. Agric. Food Chem.* **1999**, *47*, 4009−4017.

(3) Krzywicki, K. Assessment of relative content of myoglobin, oxymyoglobin and metmyoglobin at the surface of beef. *Meat Sci.* **1979**, *3*, 1−10.

(4) Zhang, A.; Wan, L.; Wu, C.; Fang, Y.; Han, G.; Li, H.; Zhang, Z.; Wang, H. Simultaneous determination of 14 phenolic compounds in grape canes by HPLC-DAD-UV using wavelength switching detection. *Molecules* **2013**, *18*, 14241−14257.

(5) Wrona, M.; Blasco, S.; Becerril, R.; Nerin, C.; Sales, E.; Asensio, E. Antioxidant and antimicrobial markers by UPLC((R))-ESI-Q-TOF-MS(E) of a new multilayer active packaging based on Arctostaphylos uva-ursi. *Talanta* **2019**, *196*, 498−509.

(6) Carpenter, R.; O'Grady, M. N.; O'Callaghan, Y. C.; O'Brien, N. M.; Kerry, J. P. Evaluation of the antioxidant potential of grape seed and bearberry extracts in raw and cooked pork. *Meat Sci.* **2007**, *76*, 604−610.

(7) Mohd Azman, N. A.; Gallego, M. G.; Segovia, F.; Abdullah, S.; Shaarani, S. M.; Almajano Pablos, M. P. Study of the properties of bearberry leaf extract as a natural antioxidant in model foods. *Antioxidants* **2016**, *5*, 1−11.

(8) Panusa, A.; Petrucci, R.; Marrosu, G.; Multari, G.; Gallo, F. R. UHPLC-PDA-ESI-TOF/MS metabolic profiling of Arctostaphylos pungens and Arctostaphylos uva-ursi. A comparative study of phenolic compounds from leaf methanolic extracts. *Phytochemistry* **2015**, *115*, 79−88.

(9) Olennikov, D. N.; Chekhirova, G. V. 6″-Galloylpicein and other phenolic compounds from Arctostaphylos uva-ursi. *Chem. Nat. Compd.* **2013**, *49*, 1−7.

(10) Kurkin, V. A.; Ryazanova, T. K.; Daeva, E. D.; Kadentsev, V. I. Constituents of Arctostaphylos uva-ursi leaves. *Chem. Nat. Compd.* **2018**, *54*, 278−280.

(11) McCullagh, M.; Douce, D.; Van Hoeck, E.; Goscinny, S. Exploring the complexity of steviol glycosides analysis using ion mobility mass spectrometry. *Anal. Chem.* **2018**, *90*, 4585−4595.

(12) Paglia, G.; Smith, A. J.; Astarita, G. Ion mobility mass spectrometry in the omics era: Challenges and opportunities for metabolomics and lipidomics. *Mass Spectrom. Rev.* **2021**, *1*, 44.

(13) Bauer, A.; Luetjohann, J.; Hanschen, F. S.; Schreiner, M.; Kuballa, J.; Jantzen, E.; Rohn, S. Identification and characterization of pesticide metabolites in Brassica species by liquid chromatography travelling wave ion mobility quadrupole time-of-flight mass spectrometry (UPLC-TWIMS-QTOF-MS). *Food Chem.* **2018**, *244*, 292−303.

(14) Canellas, E.; Vera, P.; Nerín, C. Ion mobility quadrupole time-of-flight mass spectrometry for the identification of non-intentionally added substances in UV varnishes applied on food contact materials. A safety by design study. *Talanta* **2019**, *205*, 120103.

(15) Claassen, C.; Ebel, E.; Kuballa, J.; Rohn, S. Impacts of fungicide treatment and conventional fertilization management on the potato metabolome (Solanum tuberosum L.) evaluated with UPLC-IMS-QToF. *J. Agric. Food Chem.* **2019**, *67*, 11542−11552.

(16) Dodds, J. N.; Hopkins, Z. R.; Knappe, D. R. U.; Baker, E. S. Rapid characterization of per- and polyfluoroalkyl substances (PFAS) by ion mobility spectrometry-mass spectrometry (IMS-MS). *Anal. Chem.* **2020**, *92*, 4427−4435.

(17) Qi, W.; Wang, Y.; Cao, Y.; Cao, Y.; Guan, Q.; Sun, T.; Zhang, L.; Guo, Y. Simultaneous analysis of fatty alcohols, fatty aldehydes, and sterols in thyroid tissues by electrospray ionization-ion mobility-

mass spectrometry based on charge derivatization. *Anal. Chem.* **2020**, *92*, 8644−8648.
(18) D'Atri, V.; Causon, T.; Hernandez-Alba, O.; Mutabazi, A.; Veuthey, J. L.; Cianferani, S.; Guillarme, D. Adding a new separation dimension to MS and LC-MS: What is the utility of ion mobility spectrometry? *J. Sep. Sci.* **2018**, *41*, 20−67.
(19) Hinnenkamp, V.; Klein, J.; Meckelmann, S. W.; Balsaa, P.; Schmidt, T. C.; Schmitz, O. J. Comparison of CCS values determined by traveling wave ion mobility mass spectrometry and drift tube ion mobility mass spectrometry. *Anal. Chem.* **2018**, *90*, 12042−12050.
(20) Stow, S. M.; Causon, T. J.; Zheng, X.; Kurulugama, R. T.; Mairinger, T.; May, J. C.; Rennie, E. E.; Baker, E. S.; Smith, R. D.; McLean, J. A.; Hann, S.; Fjeldsted, J. C. An interlaboratory evaluation of drift tube ion mobility-mass spectrometry collision cross section measurements. *Anal. Chem.* **2017**, *89*, 9048−9055.
(21) Righetti, L.; Dreolin, N.; Celma, A.; McCullagh, M.; Barknowitz, G.; Sancho, J. V.; Dall'Asta, C. Travelling wave ion mobility-derived collision cross section for mycotoxins: Investigating interlaboratory and interplatform reproducibility. *J. Agric. Food Chem.* **2020**, *68*, 10937−10943.
(22) Zhou, Z.; Luo, M.; Chen, X.; Yin, Y.; Xiong, X.; Wang, R.; Zhu, Z.-J. Ion mobility collision cross-section atlas for known and unknown metabolite annotation in untargeted metabolomics. *Nat. Commun.* **2020**, *11*, 4334.
(23) Gonzales, G. B.; Smagghe, G.; Coelus, S.; Adriaenssens, D.; De Winter, K.; Desmet, T.; Raes, K.; Van Camp, J. Collision cross section prediction of deprotonated phenolics in a travelling-wave ion mobility spectrometer using molecular descriptors and chemometrics. *Anal. Chim. Acta* **2016**, *924*, 68−76.
(24) Stander, M. A.; Van Wyk, B.-E.; Long, H. S.; Long, H. S. Analysis of phenolic compounds in Rooibos Tea (Aspalathus linearis) with a comparison of flavonoid-based compounds in natural populations of plants from different regions. *J. Agric. Food Chem.* **2017**, *65*, 10270−10281.
(25) Venter, P.; Causon, T.; Pasch, H.; de Villiers, A. Comprehensive analysis of chestnut tannins by reversed phase and hydrophilic interaction chromatography coupled to ion mobility and high resolution mass spectrometry. *Anal. Chim. Acta* **2019**, *1088*, 150−167.
(26) Masike, K.; de Villiers, A.; Hoffman, E. W.; Brand, D. J.; Causon, T.; Stander, M. A. Detailed phenolic characterization of Protea pure and hybrid cultivars by liquid chromatography-ion mobility-high resolution mass spectrometry (LC-IM-HR-MS). *J. Agric. Food Chem.* **2020**, *68*, 485−502.
(27) Schroeder, M.; Meyer, S. W.; Heyman, H. M.; Barsch, A.; Sumner, L. W. Generation of a collision cross section library for multi-dimensional plant metabolomics using UHPLC-trapped ion mobility-MS/MS. *Metabolites* **2019**, *10*, 13.
(28) Waters Corporations. Natural Products Profiling CCS Library. URL https://marketplace.waters.com/apps/255816/natural-products-profiling-ccs-library#!overview (accessed 28 June 2021).
(29) Celma, A.; Sancho, J. V.; Schymanski, E. L.; Fabregat-Safont, D.; Ibáñez, M.; Goshawk, J.; Barknowitz, G.; Hernández, F.; Bijlsma, L. Improving target and suspect screening high-resolution mass spectrometry workflows in environmental analysis by ion mobility separation. *Environ. Sci. Technol.* **2020**, *54*, 15120−15131.
(30) Saleem, A.; Harris, C. S.; Asim, M.; Cuerrier, A.; Martineau, L.; Haddad, P. S.; Arnason, J. T. A RP-HPLC-DAD-APCI/MSD method for the characterisation of medicinal Ericaceae used by the Eeyou Istchee Cree First Nations. *Phytochem. Anal.* **2010**, *21*, 328−339.
(31) Kitanov, G. M.; Nedialkov, P. T. Benzophenone O-glucoside, a biogenic precursor of 1,3,7-trioxygenated xanthones in Hypericum annulatum. *Phytochemistry* **2001**, *57*, 1237−1243.
(32) Sobeh, M.; Rezq, S.; Sabry, O. M.; Abdelfattah, M. A. O.; El Raey, M. A.; El-Kashak, W. A.; El-Shazly, A. M.; Mahmoud, M. F.; Wink, M. Albizia anthelmintica: HPLC-MS/MS profiling and in vivo anti-inflammatory, pain killing and antipyretic activities of its leaf extract. *Biomed. Chromatogr.* **2019**, *115*, 108882.
(33) Gao, S.; Zhan, Q.; Li, J.; Yang, Q.; Li, X.; Chen, W.; Sun, L. LC-MS/MS method for the simultaneous determination of ethyl gallate and its major metabolite in rat plasma. *Biomed. Chromatogr.* **2010**, *24*, 472.
(34) Sudjaroen, Y.; Hull, W. E.; Erben, G.; Würtele, G.; Changbumrung, S.; Ulrich, C. M.; Owen, R. W. Isolation and characterization of ellagitannins as the major polyphenolic components of Longan (Dimocarpus longan Lour) seeds. *Phytochemistry* **2012**, *77*, 226−237.
(35) Zhu, M.; Dong, X.; Guo, M. Phenolic profiling of Duchesnea indica combining macroporous resin chromatography (MRC) with HPLC-ESI-MS/MS and ESI-IT-MS. *Molecules* **2015**, *20*, 22463−22475.
(36) Abad-García, B.; Berrueta, L. A.; Garmón-Lobato, S.; Gallo, B.; Vicente, F. A general analytical strategy for the characterization of phenolic compounds in fruit juices by high-performance liquid chromatography with diode array detection coupled to electrospray ionization and triple quadrupole mass spectrometry. *J. Chromatogr. A* **2009**, *1216*, 5398−5415.
(37) Ablajan, K.; Abliz, Z.; Shang, X.-Y.; He, J.-M.; Zhang, R.-P.; Shi, J.-G. Structural characterization of flavonol 3,7-di-O-glycosides and determination of the glycosylation position by using negative ion electrospray ionization tandem mass spectrometry. *J. Mass Spectrom.* **2006**, *41*, 352−360.
(38) Ben Faleh, A.; Warnke, S.; Rizzo, T. R. Combining ultrahigh-resolution ion-mobility spectrometry with cryogenic infrared spectroscopy for the analysis of glycan mixtures. *Anal. Chem.* **2019**, *91*, 4876−4882.
(39) Hofmann, J.; Hahm, H. S.; Seeberger, P. H.; Pagel, K. Identification of carbohydrate anomers using ion mobility-mass spectrometry. *Nature* **2015**, *526*, 241−244.
(40) Shang, Y.; Wei, W.; Zhang, P.; Ye, B.-C. Engineering yarrowia lipolytica for enhanced production of arbutin. *J. Agric. Food Chem.* **2020**, *68*, 1364−1372.
(41) Song, X.-C.; Canellas, E.; Asensio, E.; Nerín, C. Predicting the antioxidant capacity and total phenolic content of bearberry leaves by data fusion of UV−Vis spectroscopy and UHPLC/Q-TOF-MS. *Talanta* **2020**, *213*, 120831.
(42) Shahidi, F.; Zhong, Y. Measurement of antioxidant activity. *J. Funct. Foods* **2015**, *18*, 757−781.
(43) Belova, L.; Caballero-Casero, N.; van Nuijs, A. L. N.; Covaci, A. Ion mobility-high-resolution mass spectrometry (IM-HRMS) for the analysis of contaminants of emerging concern (CECs): Database compilation and application to urine samples. *Anal. Chem.* **2021**, *93*, 6428−6436.
(44) Celma, A.; Ahrens, L.; Gago-Ferrero, P.; Hernández, F.; López, F.; Lundqvist, J.; Pitarch, E.; Sancho, J. V.; Wiberg, K.; Bijlsma, L. The relevant role of ion mobility separation in LC-HRMS based screening strategies for contaminants of emerging concern in the aquatic environment. *Chemosphere* **2021**, *280*, 130799.
(45) Hernández-Mesa, M.; Le Bizec, B.; Monteau, F.; García-Campaña, A. M.; Dervilly-Pinel, G. Collision cross section (CCS) database: An additional measure to characterize steroids. *Anal. Chem.* **2018**, *90*, 4616−4625.
(46) Hernández-Mesa, M.; D'Atri, V.; Barknowitz, G.; Fanuel, M.; Pezzatti, J.; Dreolin, N.; Ropartz, D.; Monteau, F.; Vigneau, E.; Rudaz, S.; Stead, S.; Rogniaux, H.; Guillarme, D.; Dervilly, G.; Le Bizec, B. Interlaboratory and interplatform study of steroids collision cross section by traveling wave ion mobility spectrometry. *Anal. Chem.* **2020**, *92*, 5013−5022.

https://doi.org/10.1021/acs.jafc.1c02845
J. Agric. Food Chem. 2021, 69, 10856−10868